

## Time-lapse magnetotellurics monitoring of the Theistareykir geothermal reservoir (Iceland)

Nolwenn Portier<sup>1</sup>, Pascal Sailhac<sup>1,2</sup>, Sheldon Warden<sup>3</sup>, Kemâl Erbas<sup>4</sup>, Knutur Árnason<sup>5</sup>, Ásgrímur Guðmundsson<sup>6</sup>

<sup>1</sup>IPGS (Institut de Physique du Globe de Strasbourg), Université de Strasbourg/CNRS, Bâtiment Descartes, 5 rue René Descartes 67084 Strasbourg cedex, France

<sup>2</sup>GEOPS UMR 8148 Bât. 504 rue du Belvédère 91405 Orsay cedex, France

<sup>3</sup>Hyperion Geophysical Services, 7, rue de Châtenois, Strasbourg, France

<sup>4</sup>Helmholtz Centre Potsdam GFZ German Research Centre for Geosciences, Telegrafenberg, 14473 Potsdam, Germany

<sup>5</sup>Iceland GeoSurvey (ÍSOR), Grensásvegur 9, 108 Reykjavík, Iceland

<sup>6</sup>Landsvirkjun, National Energy Company, Háaleitisbraut 68, 103 Reykjavík, Iceland

nolwenn.portier@unistra.fr

**Keywords:** Theistareykir, time-lapse magnetotellurics monitoring, geothermal reservoir.

### ABSTRACT

Several geophysical methods can be used to monitor geothermal reservoirs and characterize the impact of stimulation or well production. A few studies have been reported using time-lapse magnetotellurics (MT) (Peacock *et al.* 2012, Abdelfettah *et al.* 2018). We present here such an experiment, conducted to monitor the geothermal reservoir of Theistareykir in Iceland. MT is sensitive to resistivity variations in the subsurface. Hence, repeated MT measurements may help identify the geothermal fluid path and characterize the evolution of the reservoir, such as alteration of the medium, or changes in water salinity or temperature.

The Theistareykir geothermal plant is located on the path of the mid-Atlantic ridge in Northeastern Iceland. A first operation phase began in autumn 2017 to produce 45 MWe and a second phase started in spring 2018 to reach a total capacity of 90 MWe. Fluids are extracted using 13 production wells 2 to 2.5km deep and then, re-injected into the reservoir. The temperature of the produced fluids varies between 280 and 330°C.

Measurements were conducted at 9 MT stations before and after the beginning of the operation to image resistivity variations caused by geothermal production. 5 components were measured simultaneously at each setup location: the horizontal electric field components (Ex, Ey), the horizontal magnetic field components (Hx, Hy) and the vertical magnetic field component (Hz). Data were recorded during 48 to 96 hours with 3 METRONIX ADU-07e stations. We used sampling rates of 512 Hz, 8,192 Hz and 65,536Hz. Filtered time series were then processed

using the Bounded Influence Remote Reference Processing (BIRRP) program to derive resistivity and phase plots (Chave and Thomson, 2004). Additionally, a continuous MT monitoring experiment was performed with 2 SPAM4 stations from the Geophysical Instrument Pool of Potsdam (GIPP), using a sampling rate of 500Hz. Our preliminary results indicate that the geothermal production increases the resistivity of the medium.

### 1. INTRODUCTION

Peacock *et al.* (2012, 2013) first used time-lapse magnetotellurics to record the impact of massive hydraulic stimulation experiments, performed at the Paralana enhanced geothermal system (EGS) in South Australia. Indeed stimulation opens existing fractures, which could induce micro-seismicity. Analyzing the stimulation induced seismic events help characterize the geothermal reservoir expansion. However, seismic data provide no information about the well connectivity, contrary to the magnetotellurics method (MT). Indeed, MT is directly sensitive to electrical resistivity contrasts. Hence, repeated measurements before and after the stimulation provide insight about fluid filled fractures. For instance, Didana *et al.* (2016) monitored the Habanero ESG stimulation in South Australia using MT: the study highlight possible conductive fractures oriented in N-S direction that is consistent with micro-seismic events measured during fluid injection. Following this work, Abdelfettah *et al.* (2018) studied the efficiency of time-lapse and continuous magnetotellurics survey to monitor the Rittershoffen plant in France during hydraulic stimulation experiment. They showed the limit of this monitoring method, which is strongly dependant of the disturbances of the Earth's magnetic field.

We applied the time-lapse and continuous MT method at the Theistareykir geothermal plant in Northeastern

Iceland. The National Power Company of Iceland, Landsvirkjun, operates the Theistareykir power station, located at the boundary between the North American and the Eurasian tectonic plates. The first exploration drilling in 2002 confirmed the promising reservoir potential, foreseen in the geothermal plant project developed in 1999. Consequently, the construction of the plant started in April 2015. The first and second power production phases began in autumn 2017 and spring 2018, respectively, to reach a total capacity of 90MWe. Hot geothermal fluids (between 280°C and 330°C) are extracted using 13 production wells 2 to 2.5km deep and then, re-injected in the ground. Repeated MT surveys will ultimately help us identify the geothermal fluid path and characterize the evolution of the Theistareykir reservoir, such as alteration of the medium, or changes in water salinity or temperature. In this extended abstract, we will only show the time-lapse MT results obtained with a sampling rate of 512Hz.

passive technique relies on simultaneous measurements of the natural electric  $E$  [V/m] and magnetic  $B$  [A/m] fields.

### 2.1 Acquisition

To cover the geothermal field, we investigated 9 MT sites before and after the beginning of the power production (Fig. 1). These sites are close or co-located to MT stations already measured by ISOR between 2009 and 2012 (Kahwa, 2012; Karlsdóttir *et al.*, 2012). Recordings were carried out using METRONIX ADU-07e data loggers, MFS-06 and CM13 probes for the horizontal and vertical components respectively, and EFP-06 non-polarizable electrodes deployed on 50m long electrical dipoles. Data were collected with sampling rates of 512 Hz (Fig.2), 8,192 Hz and 65,536Hz during 48-96 hours.

## 2. METHOD

MT is a passive electromagnetic method allowing to study the resistivity variations with depth. This

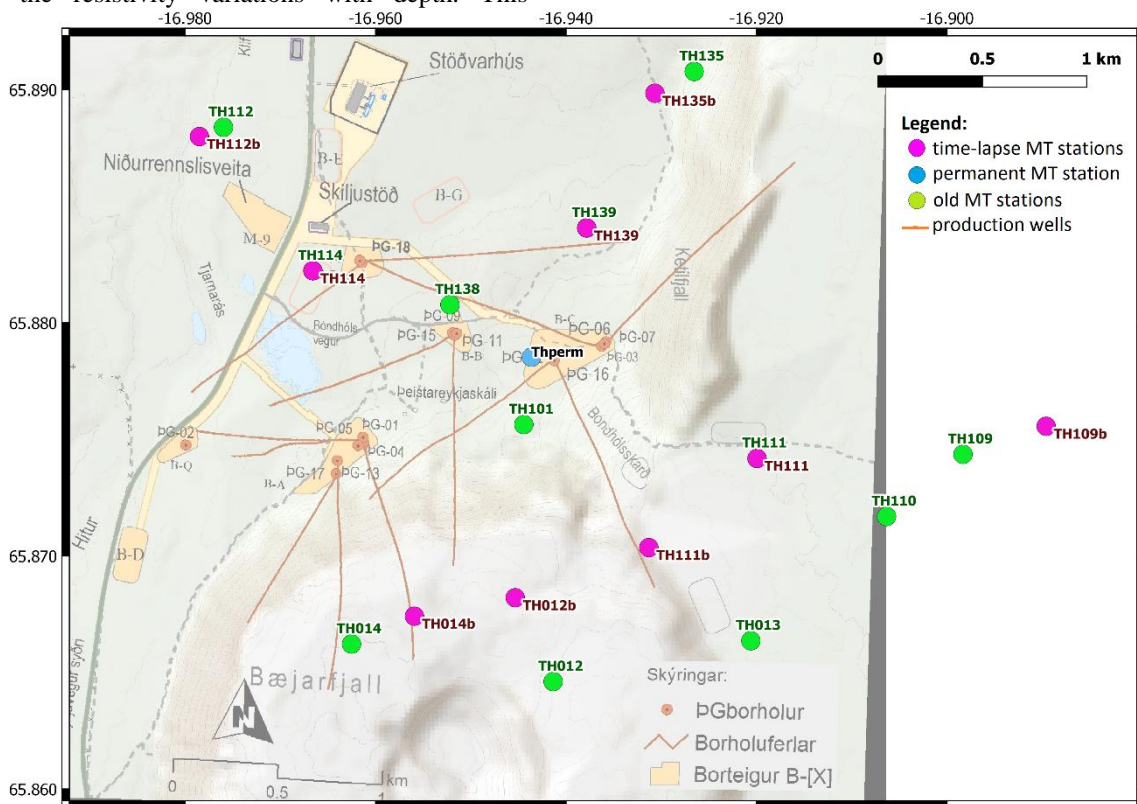
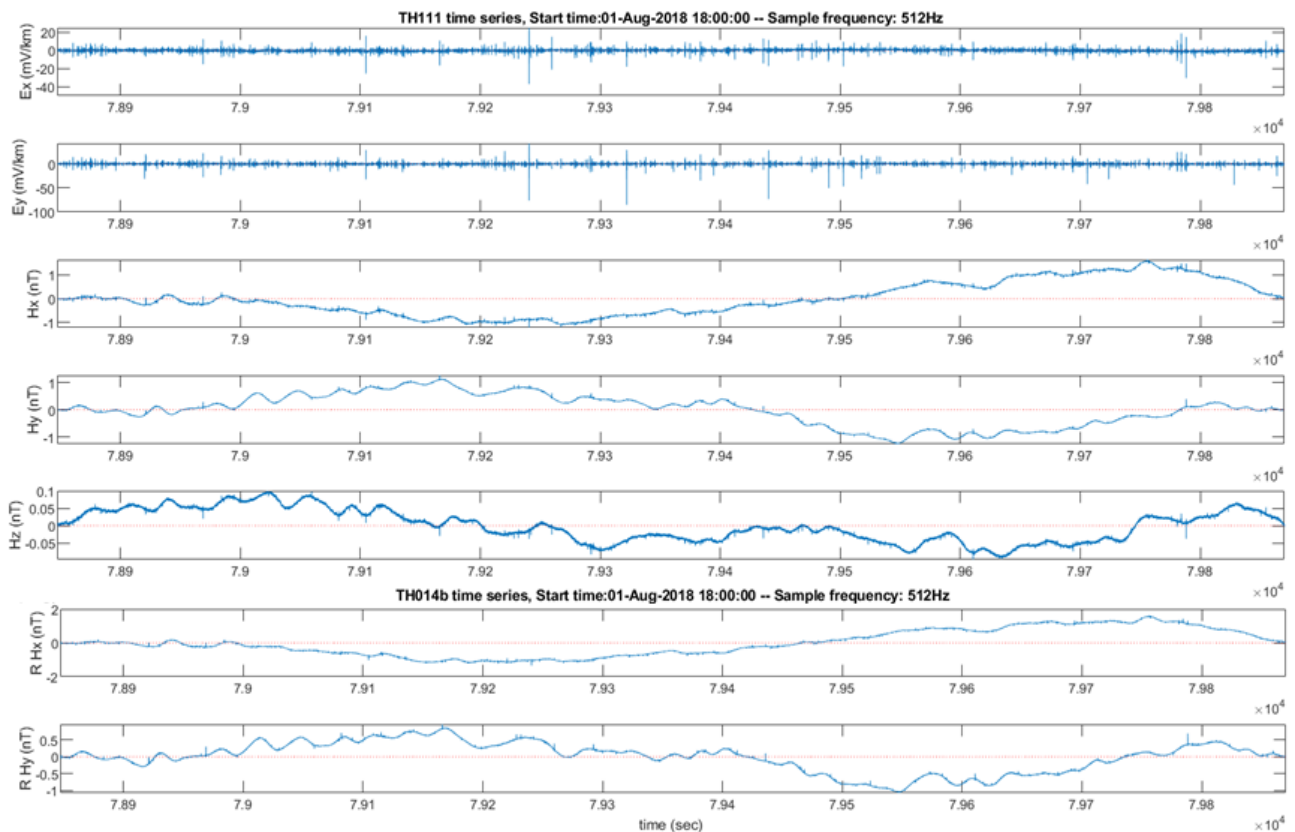


Figure 1: Map of the 10 MT stations. The semi-permanent station is depicted in blue. The 9 time-lapse stations appear in pink. We also represent the former MT stations acquired by ISOR in green. (Background map created by ISOR)



**Figure 2: 1024s time series measured at station TH111 (Ex, Ey, Hx, Hy and Hz) and remote station TH014b (R Hx, R Hy) with a sample rate of 512Hz after calibrating and filtering of 50Hz and its harmonics.**

## 2.2 Data processing

The impedance tensor  $Z$  links the horizontal components (Hx, Hy) of the magnetic field  $H$  with the horizontal components (Ex, Ey) of the electric field  $E$  [1].

$$E = ZH \quad [1]$$

To estimate the impedance phase tensor, we used the Bounded Influence Remote Reference Processing (BIRRP) program developed by Chave and Thomson (2004) on the MT data filtered from the 50Hz and its harmonics with a notched filter. Each station was processed considering a remote reference. Then, the apparent resistivity  $\rho$  [ $\Omega \cdot m$ ] and phase  $\Phi$  [degrees] are calculated using the impedance in spectral domain [2, 3].

$$\rho(\omega) = \frac{|Z|^2}{\mu\omega} \quad [2]$$

$$\Phi(\omega) = \arctan\left(\frac{\text{Im}(Z)}{\text{Re}(Z)}\right) \quad [3]$$

where  $\mu$  is the magnetic permeability [H/m] and  $\omega$  is the angular frequency [rad/s]. Hence, we obtain the sounding curves of apparent resistivity and phase versus periods. In practice, we will only consider  $Z_{xy}$  and  $Z_{yx}$  components [4,5].

$$Z_{xy} = \frac{E_x}{H_y} \quad [4]$$

$$Z_{yx} = \frac{-E_y}{H_x} \quad [5]$$

Several decimations were used: A decimation of 1, 8 and 16 were used to process periods lower than  $9 \cdot 10^{-2}$  s, periods between  $9 \cdot 10^{-2}$  s and  $3 \cdot 10^{-1}$  s and periods between  $3 \cdot 10^{-1}$  s and 3s, respectively. The periods varying between 3s and 20s were studied using a decimation of 512. Finally, the higher periods were processed using a decimation of 2048.

## 3. THE RESISTIVITY STRUCTURE

In Icelandic high-temperature geothermal systems like the Theistareykir field, the resistivity structure can be divided in four zones, from top to bottom (Árnason *et al.*; 2008, Kahwa, 2012; Karlsdóttir *et al.*, 2012):

- A resistive area characterized by unaltered rock formations (zone 1);
- The smectite-zeolite zone forming a low resistivity cap (zone 2);
- The mixed layered clay zone where resistive chlorite replaces smectite, and zeolite disappears (zone 3);
- The resistive chlorite-epidote area (zone 4).

For instance, the apparent resistivity measured at station TH109b (Fig. 3) for the low periods is greater than 100  $\Omega \cdot m$  (zone 1). It reaches a minimum of 20-30  $\Omega \cdot m$  between 0.3 s and 0.5 s (zone 2) and, then, increases up to several tens of  $\Omega \cdot m$  (zones 3 and 4).

As the borehole correlation confirmed it (Kahwa, 2012), the resistivity structure is therefore defined by the alteration mineralogy. Resistivity measurements provide information about mineral alteration and therefore the temperature that was reached in order to trigger such alteration. Resistivity gives insight about the maximum temperature to which the system was exposed throughout its history (Páll Hersir and Árnason, 2013).

#### 4. RESULTS

We superimposed sounding curves of the apparent resistivity and phase versus period obtained in 2017 (before the beginning of the power production) and in

2018 (after the beginning of the power production) at the Theistareykir geothermal plant.

##### 4.1 Undisturbed area

Station TH109b is located outside the geothermal field, to the East (Fig.1). In 2018, we processed only one day of data, allowing us to reach a period of 130s. We do not observe any changes between the 2017 and 2018 sounding curves (Fig.3), leading us to conclude that the geothermal production did not affect this station. Indeed, the soundings curves are quite regular and error bars are short including the so called “MT dead band” of low geomagnetic activity periods near 1s. We applied no interpolation or filtering to the sounding curves.

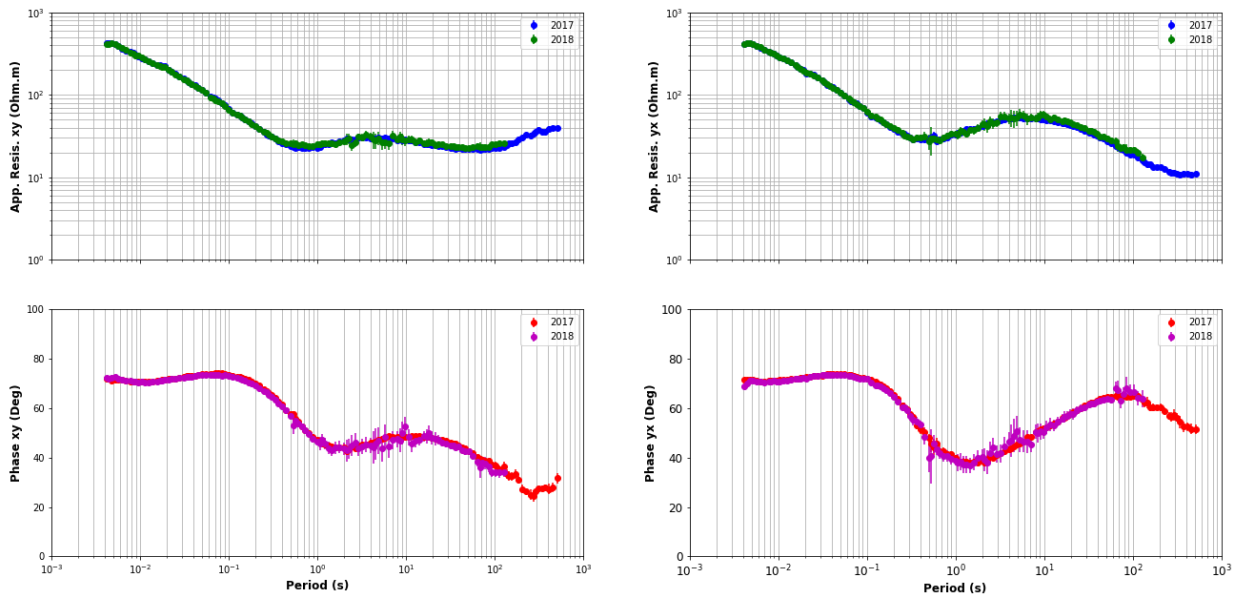


**Figure 3: Apparent resistivity and phase plots for station TH109b acquired in 2017 (blue and red curves) and in 2018 (green and purple curves).**

##### 4.2 Above the Baejarfjall volcano

Located on the Baejarfjall volcano, stations TH014b, TH012b and TH111b (Fig.1) are above production wells. In this extended abstract, we choose to only show the sounding curves of station TH014b (Fig.4). Due to a set-up problem, we did not measure the electric field Ex in 2017 at station TH012b.

Stations TH014b and TH111b show the same trend for the apparent resistivity XY. It increases in 2018 with respect to 2017 for frequencies below 5Hz and 10Hz, respectively. The correcting constant considering the

logarithmic equation is equal to  $3.3 \cdot 10^{-2} \pm 63\%$   $\Omega \cdot m$  for station TH014b and  $5.0 \cdot 10^{-2} \pm 38\%$   $\Omega \cdot m$  for station TH111b.

At stations TH014b and TH012b, the apparent resistivity YX decreases in 2018 with respect to 2017 for frequencies above 8Hz and 5Hz, respectively. The correcting constant considering the logarithmic equation is equal to  $-4.8 \cdot 10^{-2} \pm 15\%$   $\Omega \cdot m$  for station TH014b and  $-5.2 \cdot 10^{-2} \pm 7\%$   $\Omega \cdot m$  for station TH012b.

Otherwise, we do not observe any significant changes between the 2017 and 2018 soundings.

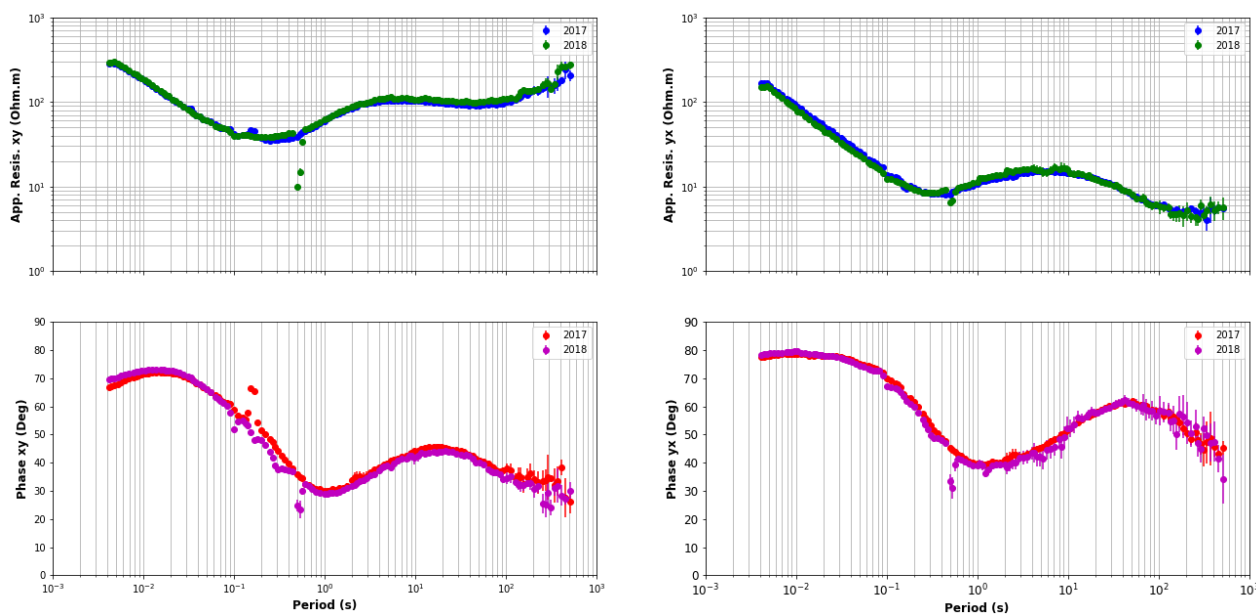


**Figure 4: Apparent resistivity and phase plots for station TH014b acquired in 2017 (blue and red curves) and in 2018 (green and purple curves).**

**4.3 North of the geothermal production**

At the north of the geothermal area (Fig.1), stations TH135b and TH139 show the strongest variations. We only show the sounding curves of station TH139 (Fig. 5). We superimposed the former results obtained by ISOR (Karlsdóttir *et al*, 2012).

The apparent resistivity YX increases in 2018 with respect to 2017 for frequencies above around 2Hz at

station TH135b. The correcting constant considering the logarithmic equation is equal to  $6.6 \cdot 10^{-2} \pm 34\%$   $\Omega \cdot m$ .

On the contrary, the apparent resistivity XY decreases in 2017 for frequencies below 3Hz (TH135b) and 5Hz (TH139). The correcting constant considering the logarithmic equation is equal to  $-5.6 \cdot 10^{-2} \pm 41\%$   $\Omega \cdot m$  for station TH135 and  $-7.5 \cdot 10^{-2} \pm 24\%$   $\Omega \cdot m$  for station TH139.

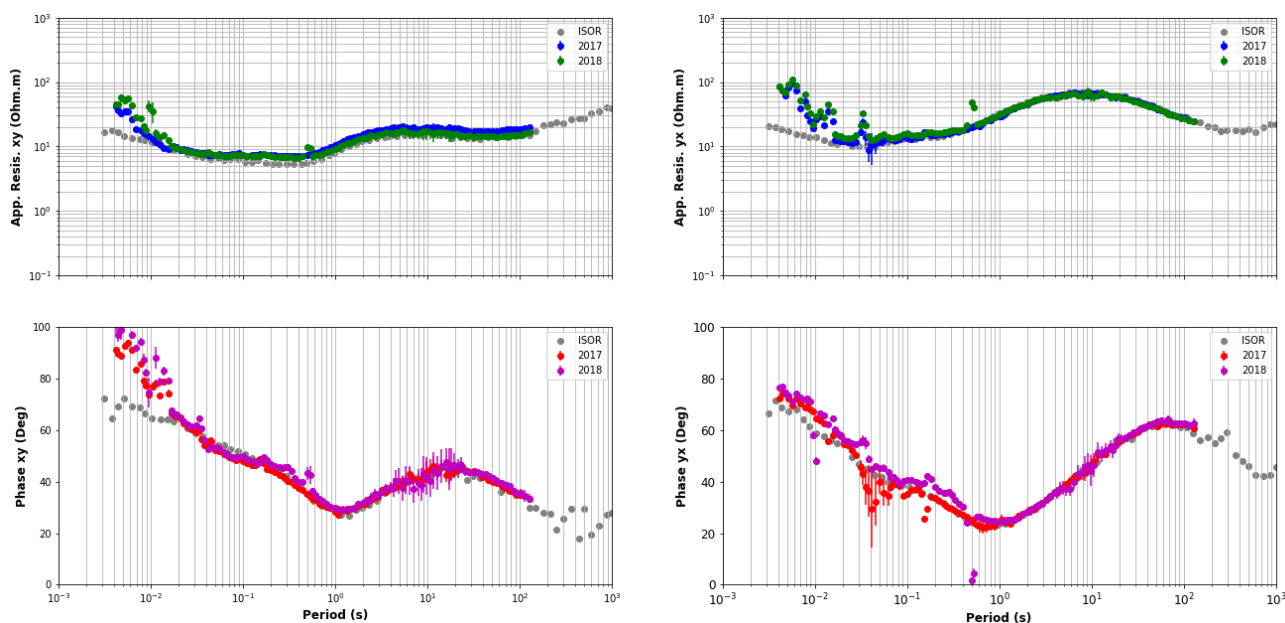


**Figure 5: Apparent resistivity and phase plots for station TH135b acquired in 2017 (blue and red curves) and in 2018 (green and purple curves). We superimposed in grey the former sounding curves obtained by ISOR (Karlsdóttir *et al*, 2012)**

**4.4 East of the geothermal production**

Stations TH112b and TH114 are close to the injection area in the western part of the geothermal field (Fig.1).

The data recorded there are noisier because of a south-north electrical line. We do not notice any clear change in the apparent resistivity. Figure 6 shows the sounding curves obtained at station TH112b.



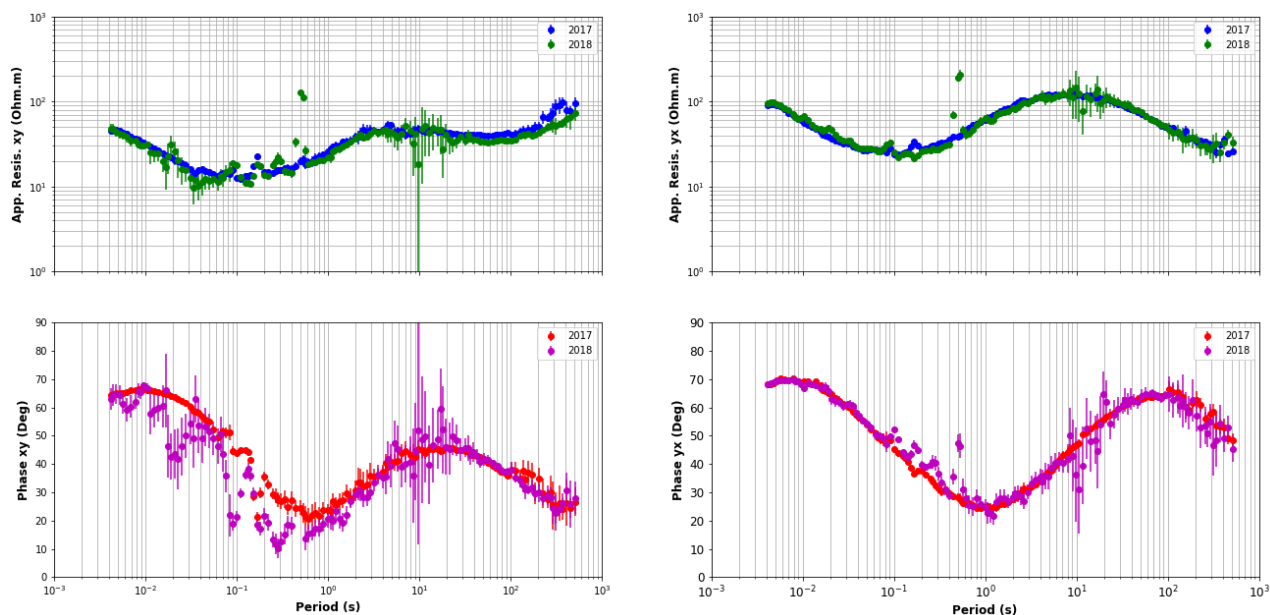


**Figure 6: Apparent resistivity and phase plots for station TH112b acquired in 2017 (blue and red curves) and in 2018 (green and purple curves).**

### 3. CONCLUSIONS

We monitored the Theistareykir geothermal reservoir using the time-lapse magnetotellurics method. We measured 9 MT stations before and after the beginning of the power production. Hence, we estimated the influence of the geothermal production on the apparent resistivity and phase. In this extended abstract, we discuss the first results with a preliminary simplistic approach; Detailed numerical modelling will be done later.

As expected, we do not observe any significant changes at station TH109b which is outside the geothermal field. Near the injection area, no clear changes in resistivity appear.

We would notice shallow significant variations in resistivity on the component yx as shown on stations TH014b, TH012b and TH135b. Variations on xy component are deeper. Indeed, we notice a decrease

on stations TH135b and TH139 and an increase on stations TH014b and TH111b in 2018 with respect to 2017. Hence, we assume the formation of a resistive structure in the north-south direction (Fig.7) that would be below stations TH014b and TH111b. Stations TH135b and TH139 should be west to this body. It could be due to the gaz supposedly created by the geothermal production which would filled the north-south fractures.

A new MT campaign will be carried out in summer 2019 to refine these results. We will also calculate the tipper and the phase tensor (Peacock *et al.* 2012, Abdelfettah *et al.* 2018) followed by a sensitivity analysis by numerical modelling. The continuous monitoring should also improve our understanding of the geothermal reservoir evolution. Futhermore, we will be able to confront the results to our gravity observations (see abstract Hybrid gravimetry monitoring of the Theistareykir and Krafla geothermal reservoirs (Iceland)).

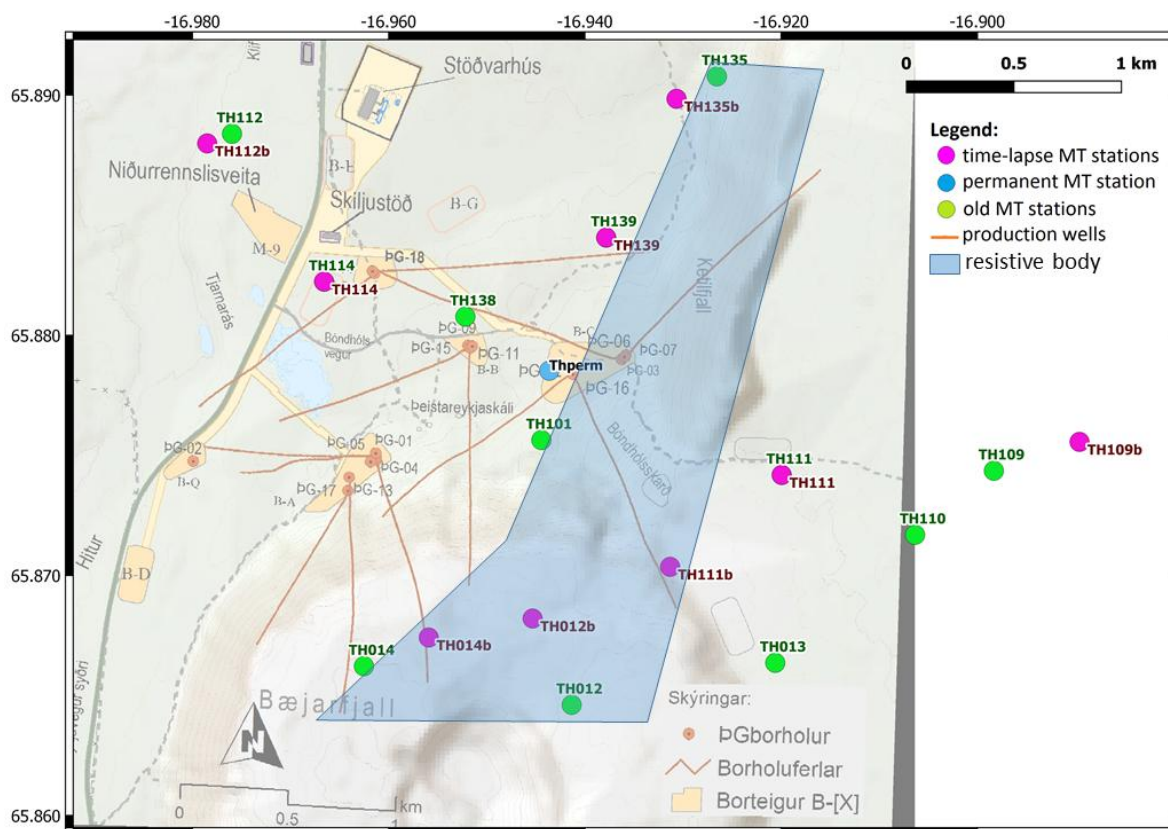


**Figure 7:** Map of the 10 MT stations. The semi-permanent station is depicted in blue. The 9 time-lapse stations appear in pink. We also represent the former MT stations acquired by ISOR in green. (Background map created by ISOR). We added the supposed resistive structure created between 2017 and 2018 (blue polygon).

## REFERENCES

- Abdelfettah, Y., Sailhac, P., Larnier, H., Matthey, P.D., Schill, E.: Continuous and time-lapse magnetotelluric monitoring of low volume injection at Rittershoffen geothermal project, northern Alsace-France. *Geothermics* (2018) 71: 1-11
- Árnason K., Flóvenz Ó., Georgsson L.S., Hersir, G.P.: Resistivity structure of high temperature geothermal systems in Iceland. *International Union of Geodesy and Geophysics (IUGG) XIX General Assembly*, (1987) Vancouver Canada, Abstracts V, 477
- Chave, A.D. and Thomson, D.J.: Bounded influence magnetotelluric response function estimation. *Geophysical Journal International* (2004) 157: 988-1006
- Didana, Y.L., Heinson, G., Thiel, S., Krieger, L. Magnetotelluric monitoring of permeability enhancement at enhanced geothermal system project. *Geothermics* (2016) 66: 23-38
- Kahwa E.: Geophysical exploration of high-temperature geothermal areas using resistivity methods-case study: Theistareykir area, NE-Iceland. *Report 14 in: Geothermal training in Iceland 2012. UNU-GTP*, (2012), 235-263.
- Karlsdóttir, R., Vilhjálmsson, A.M., Árnason, K., Beyene, A.T.: Theistareykir Geothermal Area, Northern Iceland 3D- Inversion of MT and TEM Data, *ISOR-2012/046 Project* (2012) 7000/12.
- Páll Hersir, G., Árnason, K.: Resistivity of rocks. *In: Short Course VIII on Exploration for Geothermal Resources*, Kenya (2013)
- Peacock, J.R., Thiel, S., Reid, P., Heinson, G.: Magnetotelluric monitoring of a fluid injection: Example from an enhanced geothermal system. *Geophys. Res. Lett.* (2012) 39: L18403
- Peacock, J.R., Thiel, S., Heinson, G., Reid P: Time-lapse magnetotelluric monitoring of an enhanced geothermal system. *Geophysics* (2013) 78: B121-B130

## Acknowledgements

We thank the Landsvirkjun (The National Power Company of Iceland), ISOR (Iceland Geosurvey) and GFZ (German Research Centre for Geosciences) for the close collaboration, the information exchange and continued support. This work has been carried out under the framework of the LABEX ANR-11-LABX-0050\_G-EAU-THERMIE-PROFONDE and benefits from a State funding managed by the French National Research Agency as part of the Investments for the Future program.